

Impact of Realistic Light Radiation Pattern on Vehicular Visible Light Communication

Agon Memedi*, Hsin-Mu Tsai†, Falko Dressler*

*Heinz Nixdorf Institute and Dept. of Computer Science, Paderborn University, Germany

†Dept. of Computer Science and Information Engineering, National Taiwan University, Taipei, Taiwan
{memedi,dressler}@ccs-labs.org, hsinmu@csie.ntu.edu.tw

Abstract—We investigate the impact of realistic light radiation pattern on Vehicular VLC (V-VLC) based on an empirical study for typical car headlight and taillight modules. Our research community identified visible light as a communication technology that has a number of advantages to radio communication. Besides the huge spectrum that is fully unlicensed, the technology allows for very high data rates and reduced interference from parallel communications. After seeing a number of breakthroughs in indoor environments, the vehicular networking community got interested in the technology for a number of reasons as well. First successful applications have been reported but practical evidence is still limited. This is due to the use of very abstract simulation models and limited field testing as of now. We aim at bridging this gap by developing a realistic simulation model based on empirical data from a measurement campaign. Based on this model, we particularly investigate the impact of the light radiation pattern of typical car light modules on the communication performance. We can report that the angle and distance of the communicating cars have a significant impact and need to be carefully considered for developing V-VLC applications.

I. INTRODUCTION

Driven by the rapid development of solid state lighting technologies and the quick adoption of Light Emitting Diodes (LEDs) as primary source of illumination in different setups, Visible Light Communication (VLC) has emerged as a potential complementary technology for data communications [1]. Most of the earlier works on VLC have considered its deployment in indoor scenarios, thus, substantial progress has been achieved on that front. For example, first generation VLC-enabling commercial products, such as pureLiFi™, are already available on the market, while standardization efforts are actively taking place in the scope of IEEE standards association [2].

Although the same does not hold true for outdoor scenarios, recent works have shown promising results [3]. One of the main outdoor applications for VLC are Intelligent Transportation Systems (ITSs) [4], [5], [6]. There is a trend towards LED-based lighting modules in the automotive industry and, thus, Vehicular VLC (V-VLC) is becoming a viable technology for vehicular networking. The vehicular environment has specific properties which differ from other scenarios. Most notably, it is characterized by a dynamic environment with high node mobility and frequently changing network topology.

Compared to Radio Frequency (RF) communication technologies, such as Dedicated Short Range Communication (DSRC) and Long Term Evolution (LTE), which are tradi-

tionally considered for vehicular networks, VLC offers many advantages [5], [7]. For instance, due to the directional nature of VLC the interference from other communicating nodes is confined, as opposed to the aforementioned omni-directional RF communications. From the security perspective, its intrinsic requirement for Line Of Sight (LOS) makes for a secure communication since potential attacks intercepting the LOS cannot go unnoticed [8]. Furthermore, VLC has a license-free spectrum orders of magnitude larger than the RF band, allowing data-rates up to Gigabit per second speeds over small and medium distances [9].

A considerable number of publications have addressed V-VLC related topics in the past few years, including channel modeling, propagation characteristics and potential applications. However, a large portion of those studies, especially those dealing with higher layer protocols, are based on strong assumptions regarding important aspects of V-VLC such as communication range and headlight/taillight radiation pattern.

We address exactly these questions in this paper and present a V-VLC simulation model for realistic headlight and taillight radiation pattern. The presented model is based on empirical data obtained from a measurement campaign conducted, in part, in a previous study [10]. We integrated the model with the popular vehicular network simulation framework Veins [11] and made it publicly available as Open Source.¹ Based on the empirical model, we investigated the impact of radiation pattern of a typical car's LED-based headlight and taillight on the communication performance. For this, we performed extensive simulations for relevant scenarios and evaluated the performance of V-VLC. We see this study as a first step towards protocol developments based on empirical evidence about the impact of the light radiation pattern.

Our key contributions can be summarized as follows:

- We developed a novel V-VLC simulation model based on very accurate empirical data allowing realistic simulation of V-VLC in ITS scenarios.
- We investigated the impact of car lighting module radiation pattern on the communication of vehicles on the same lane as well as on different lanes.
- We further shed light on the impact of curved roads on the V-VLC channel and the impact on connectivity under such conditions.

¹<http://ccs-labs.org/software/>

II. RELATED WORK

A. Channel Modeling

One of the most comprehensive studies addressing channel modeling for Vehicle-to-Vehicle (V2V) applications based on VLC technology was conducted by Luo et al. [12]. The authors use analytical methods to model a wide range of factors in such a system. They characterize the daylight beam pattern of empirically measured low and high beams of LED headlights selected based on vehicle sale numbers. On the receiving side, their model accounts for the LOS and Non LOS (NLOS) components of the signal, including the implications of the road surface on NLOS reflections. Thermal noise, solar shot noise, and receiver characteristics are considered as well. Although the presented mathematical model is comprehensive, it was not validated empirically.

In contrast, Turan et al. [13] use empirical methods to investigate the feasibility of LOS Multiple-Input Multiple-Output (MIMO) communication realized via vehicle taillights. They obtain a realistic channel model through measurements for each of the taillights and then use various modulation schemes for four taillight-MIMO configurations to achieve the highest Signal-to-Noise Ratio (SNR). Amongst others, their findings show that using all of the taillights is not the best option due to distribution of the power on the transmitter side when they are driven by the same hardware concurrently.

Chen et al. [14] use real-world traces collected from a car-following scenario to characterize the time variation of the VLC channel between the receiving vehicle in the front and the transmitting headlight of the following vehicle. Results show that turning maneuvers account for significant variations in received optical power in the V-VLC channel. This is attributed to the change of important path loss factors such as distance, irradiance and incidence angles during such maneuvers. It is also shown that vertical movements of the vehicles, caused by road irregularities, have intermittent but non-trivial effects on the received optical power.

Miramirkhani et al. [15] use a commercially available simulation tool to study the path loss and delay spread of indoor VLC channel in the presence of mobile users. CAD models are used to design the scenario, and detailed reflection characteristics of the environment, including walls, floor, ceiling, furniture, and humans are specified for simulation. Using ray tracing techniques the authors show that there are significant fluctuations in the received power caused by human mobility. To combat this, an adaptive scheme aiming to maximize SNR by selecting optimal transmitter and modulation order combination is proposed.

B. V-VLC Applications

V-VLC has been considered for different applications in the context of vehicular networking. Segata et al. [6] study the impact of combining VLC and DSRC to realize platooning. VLC is used as a secondary channel for offloading some of the network traffic. Although the authors show that VLC would be beneficial in such applications, the VLC channel they use is purely probabilistically modeled and, thus, rather unrealistic.

Similarly, Ishihara et al. [16] combine VLC and DSRC in the scope of a platooning application. They address the problem of RF jamming in a platooning application and point out that directional VLC channel can be used for sharing safety-critical messages, which otherwise could be compromised in case of jamming attacks on the radio channel.

A different category of V-VLC applications focusses on Vehicle-to-Infrastructure (V2I) communication. For instance, Yamazato et al. [17] propose a positioning application that deploys high-speed cameras to infer the position of vehicles while transmitting VLC signals along the same channel. Another V2I application is suggested by Kumar et al. [18]: Here, traffic lights are integrated to the ITS infrastructure and used for data communication with the vehicles via VLC.

III. CHANNEL MODELING FOR V-VLC SIMULATION

In the following, we first introduce the measurement data, which forms the basis of our model, and then establish the V-VLC model for realistic V-VLC simulation.

A. Empirical Measurements

We use empirical data of measured headlight and taillight radiation patterns to design our channel model as realistically as possible. The measurement data has been collected in part for a previous study by Tseng et al. [10], where the authors use a vehicle's left headlight and taillight during a measurement campaign. Both of the lighting modules are based on LED technology. During the measurements only the low beam is used for the headlight, whereas for the taillight they utilize both the positioning and the brake light. On the receiving end of their VLC communication system, an off-the-shelf Photodiode (PD) was used. The measurements were performed at night in a stationary setting to minimize the influence of environmental factors. To determine the measurement points, first the distance between the transmitting light module and the PD was specified. Then, ten measurement points were uniformly distributed in that distance. This process was iterated for multiple angles between the receiver and the transmitter, until the radiation pattern of the given lighting module is fully covered. Further information including technical details of the experiment and the used hardware setup can be found in [10].

Figure 1 shows the radiation pattern of the measured electrical Received Signal Strength (RSS) for each of the lighting modules. In essence, we have a birds-view perspective of the emitted light beams. The relative location of the light source is plotted at 0 m. On the horizontal axis, we see the distribution of optical power on the sides of the light source, whereas, on the vertical axis, we see the lengthwise distribution of the optical power relative to the light source. Contour lines are drawn each time the measured RSS crosses a boundary of 10 dBm. This helps us to understand the spatial distribution of the optical power. Note that for both the headlight and the taillight, the last contour line is drawn at -114 dBm. That is because at the time of the measurements, the ambient noise was equal to -114 dBm. Practically, this is the value where the light source could no longer be detected by the PD.

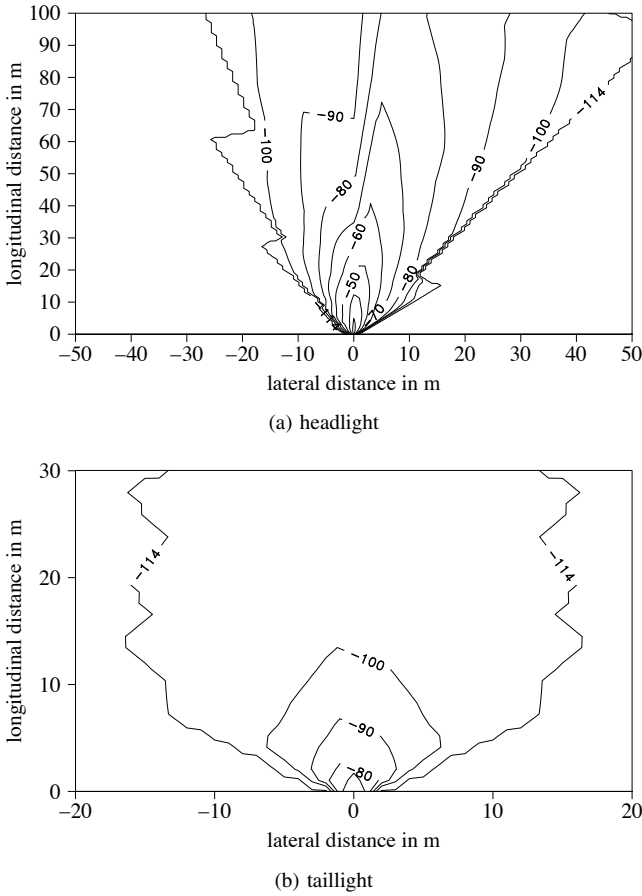


Figure 1. Radiation pattern of LED-based headlight and taillight modules given in dBm. The RSS values on the contour lines denote the lower bound for the corresponding region.

Figure 1a shows the radiation pattern of the headlight. We can see that the RSS has weaker concentration on the left side of the emitted light beam. This is due to lighting regulations mandating slightly dimmer light in the direction of the opposite traffic. The idea is to minimize the potential disturbance of the drivers on the opposing lanes. This asymmetric distribution of the power is relevant for our path loss modeling of the headlight later on. From Figure 1b we see that the taillight's radiation pattern is more symmetric. Note that the headlight and the taillight have different axis limits. This points out the significant difference in potential communication range.

B. Model Fitting

In the following, we present the model fitting process for integrating the empirical data in a simulation framework. Due to the limited space, we only discuss the headlight, also motivated by its unorthodox radiation pattern and better communication range compared to the taillight. We used the non-linear least squares method and the surface fitting tool from the Curve-fitting toolbox of MATLAB for deriving the following equations. Characterizing the path loss between the transmitter and the receiver is first based on the distance:

$$P_{\text{distance}}[\text{dBm}] = \alpha + 10 \times \beta \times \log_{10} \left(\frac{1}{\text{distance} + \gamma} \right). \quad (1)$$

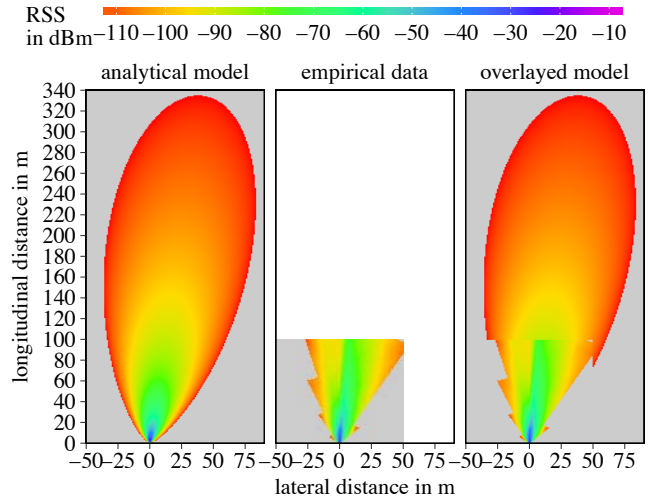


Figure 2. Comparison of the derived model, the empirical data, and the combination of both.

We derived $\alpha = 695.3$, $\beta = 4.949$, and $\gamma = 1$ from our empirical data. Secondly, the angle of the communicating parties needs to be considered:

$$P_{\text{angle}}[\text{dBm}] = \delta + \epsilon \times \cos \left(\frac{2 \times \pi \times (\text{angle} + 90)}{\omega} \right). \quad (2)$$

Here, we obtained $\delta = -747.3$, $\epsilon = 63.13$, and $\omega = 173$ from our empirical data. The fitting parameters for Equations (1) and (2) were determined empirically and we achieved a goodness of fit characterized by $R^2 = 0.8703$.

Finally, we can compute the RSS for a given distance and angle between transmitter receiver as

$$P_{\text{total}}[\text{dBm}] = P_{\text{distance}}[\text{dBm}] + P_{\text{angle}}[\text{dBm}], \quad (3)$$

assuming that the receiver is within LOS of the transmitter.

Figure 2 shows three plots of the radiation pattern of the headlight. Instead of using contour lines to visualize the RSS, we now use colors to represent different RSS values. The plot on the left shows RSS values as calculated using the derived analytical model. For comparison, we show the RSS from the empirical data in the middle plot. We observe that Equation (3) closely models the empirical data, particularly the asymmetric angular behavior manifested with weaker concentration of power on the left side of the headlight. Moreover, we can calculate RSS values for distances beyond the limits of the empirical data and extend to longitudinal and lateral distances of 330 m and 75 m, respectively. We discuss the plot on the right in the following subsection.

C. Implementation and Validation

We finally implemented the empirical model in the Veins simulator [11], which is very popular in the vehicular networking research community. We extend the tool with an additional module to enable V-VLC. For the headlight, we overlay the empirical model and the analytical model.² More specifically,

²In simulation, the empirical data accounts for the incidence angle between the transmitter and receiver; the analytical model does not.

we give precedence to values from the measurements for the points within its scope and use the analytical model for the points beyond, as shown in the rightmost plot in Figure 2. As can be seen, there are regions in the overlay model, where the signal strength experiences rapid changes. This is a side-effect of combining empirical data and the analytical model. The effect is most noticeable in the boundaries of the empirical data, e.g., at distances between 90 to 110 m and -40 to -25 m for the longitudinal and the lateral planes, respectively. The statistical correctness is not influenced even though single measurements may slightly deviate. To simulate the V-VLC via taillight, we use only the empirical data due to the simpler pattern and shorter communication range.

We also comply with the IEEE 802.15.7 [2] standard and use a PHR of 58 bit and PSDU of 65 535 bit (8192 B) for our packets. 8192 B is the maximum payload size allowed in the standard, hence, we use that value to refer to the worst case.

To model data transmission for the V-VLC channel, we assume a passband system realized with Intensity Modulation and Direct Detection (IM/DD) technique, modulating data using On-Off Keying (OOK). OOK is a binary modulation scheme where the logical 1 is represented with high level of current and the logical 0 with lower level of current. In order to avoid flickering, Manchester coding could be used. OOK is a typical modulation scheme for VLC also proposed in the specification of PHY I and PHY II in IEEE 802.15.7 [2].

The theoretical Bit Error Rate (BER) of OOK in an Additive White Gaussian Noise (AWGN) channel is given as [12]:

$$\text{BER} = Q(\sqrt{\text{SNR}}), \quad (4)$$

where $Q(x)$ is the Q-function used to calculate the tail probability of standard Gaussian distribution.

The Packet Delivery Ratio (PDR) can be derived (assuming independent bit errors and no forward error correction):

$$\text{PDR} = (1 - \text{BER})^{n\text{bits}}, \quad (5)$$

where $n\text{bits}$ stands for the bitlength of the transmitted packet.

IV. IMPACT OF RADIATION PATTERN

In a first step, we assess the impact of the angle on the V-VLC communication performance. Figure 3 illustrates the scenario modeling a road with three lanes. The reference vehicle in the middle transmits VLC packets to the front using its headlights and to the back using its taillights. All other cars try receiving the messages. The inter-vehicle distance along the vertical axis is fixed to 3.75 m, which is the typical lane-to-lane distance for urban roads in Germany. The distance along the horizontal axis is modified between 1–400 m for different simulation experiments. Additionally, the reference vehicle is rotated between -90 – 90° around its axis, to capture the effect of turning maneuvers while driving.

Figure 4 shows the probability of reception of packets transmitted by the headlight with and without payload. We plot the SNR on the horizontal axis and the PDR on the vertical axis. For packets without payload, the communication is almost perfect for SNR values greater than 11 dB. The

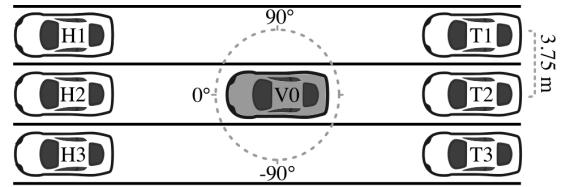


Figure 3. Road scenario with three lanes. The reference vehicle V0 transmits VLC packets. It can be rotated around its axis between -90 – 90° .

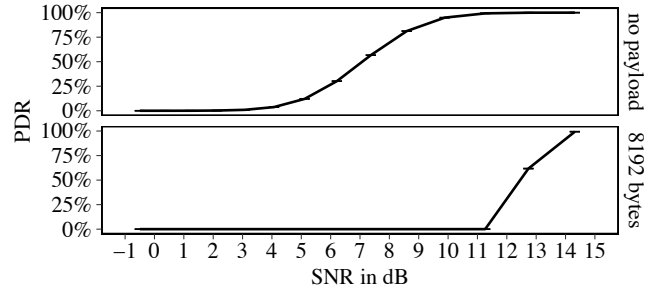


Figure 4. PDR as function of the SNR for packets transmitted via the headlight. PDR for packets without a payload is given in the upper plot, while for packets with payload of maximum size in the lower plot.

opposite is holds for SNR values smaller than 3 dB. However, this is not true for the more realistic cases where the packets have a large payload. In this case, the switch from 0 % PDR to 100 % PDR happens in a much smaller range, hence the curve is much steeper. There, slight increase in the SNR, between 11 dB and 14 dB, improves the PDR rapidly. The communication only becomes ideal for SNR larger than 14 dB. We do not show separate results for the taillight as the model only accounts for RSS values, hence the same applies.

Figure 5 shows the PDR for the packets with payload transmitted via the headlight of the reference vehicle to all cars in front of it. On the horizontal axis, we plot the distance between the reference V0 and cars H1, H2, and H3. For each of the receiving vehicles, the plots are grouped in columns. Horizontally, the plots are grouped into rows based on the heading angle of V0 at transmission time.

First, we consider the case when V0 is perfectly aligned with the other vehicles, i.e., at 0° . In this setup, V0 can communicate without a problem with all of the vehicles in front of it and up to a distance of 120 m. Due to the radiation pattern of the headlight, the communication is slightly better with H1 as it lays on the right side of V0, where the signal strength is higher. If V0 is tilted at -10° to its left, the communication range improves with all of the neighbors, because now the stronger part of headlight's radiation covers all of the neighbors. The opposite is experienced at 10° tilt to the right. At -20° , V0 can communicate reliably up to 80 m with the vehicles in all three lanes. However, beyond that angle the communication drops completely for H1, as it falls out of headlight's radiation pattern. The angular span is less for angles on the right side of H1, where the communication with H3 is already impossible at 20° . An interesting effect is observed at 1 m communication range. There, due to the directionality of VLC, V0 cannot communicate with H1 and

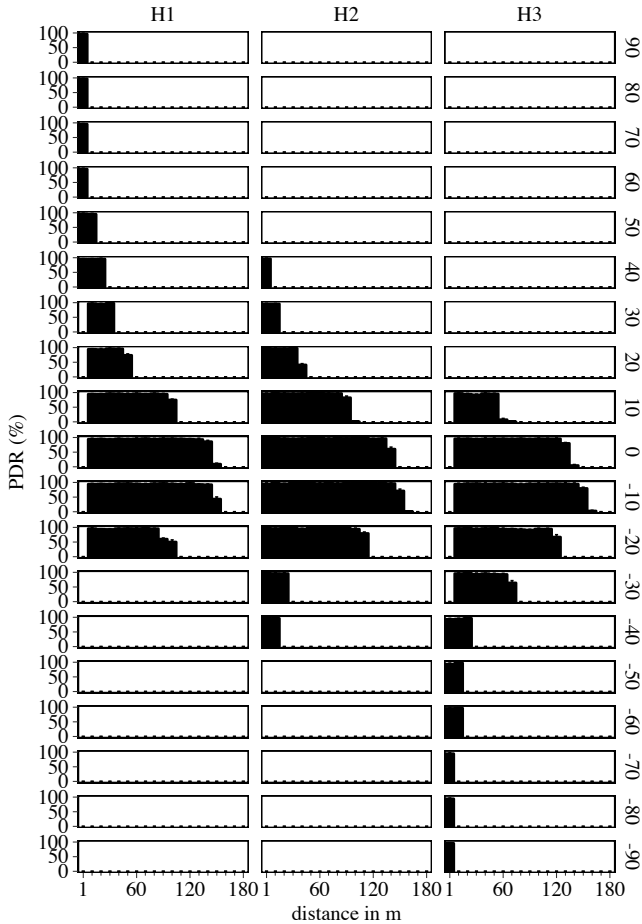


Figure 5. PDR for the vehicles in front of the reference vehicle.

H3, which are not on the same lane with it. Communication with those vehicles becomes possible only at 40° , which is in the direction of the respective vehicle.

In summary, we see that the headlight allows communication with vehicles on neighboring lanes for angles between -20 – 10° , given that the inter-vehicle distance is large enough so that the vehicle on the same lane does not absorb the complete radiation of the headlight.

We also studied the same effect for the taillight, and found out that communication with T1, T2, and T3 is only possible up to 10 m at 0° . Any change in the angle of V0 results in communication outage with the lane in the opposite of the angular rotation. The problem of taillight’s communication range has also been addressed in [13].

V. IMPACT OF CURVES ON THE ROAD

In a second set of experiments, we aim at exploring the impact of the light radiation pattern on realistic traffic along curved roads. Figure 6 illustrates the used scenario. We constructed a single-lane road consisting of three 2 km straight segments and two turns. The turns have a radius of 200 m. The idea is to show the implications of different angles of communication between the transmitter and the receiver

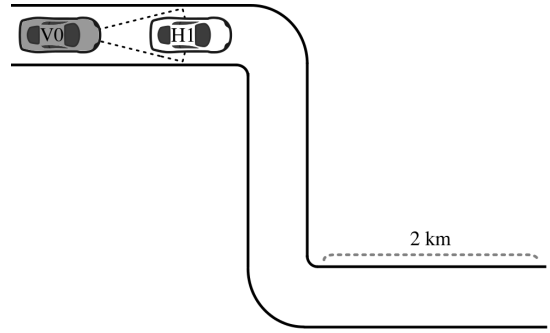


Figure 6. Road scenario with two vehicles driving. The reference vehicle V0 transmits via its headlight.

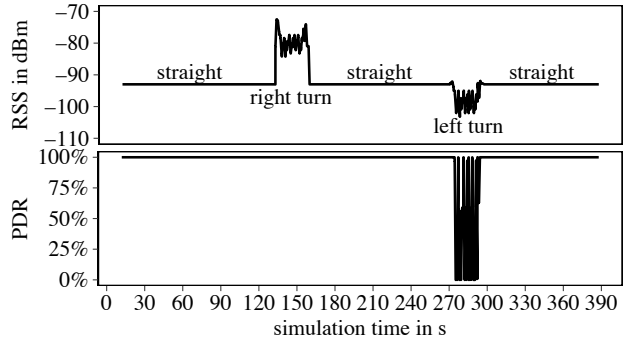


Figure 7. Time series plot for the RSS and PDR for received packets as the vehicles drive along the straight road and the curves.

as they drive through the turns. Hence, the vehicles should experience two perfectly symmetrical turns.

As far as the traffic is concerned, we deploy two vehicles following each other modeled using the SUMO simulator part of Veins. The vehicles are inserted to the scenario at the upper left road segment. The inter-vehicle distance is set to 80 m, a reasonable distance for realistic highway scenarios. We have also disabled randomness of driver behavior in SUMO in order to not affect the inter-vehicle distance. Nonetheless, there are slight fluctuations in the distance as the vehicles go through the turns, but the fluctuations are less than 40 cm and, thus, negligible. Both vehicles are capable of VLC communication, but only the vehicle in back transmits via its headlight. The transmitted packets again contain a payload of 8192 B.

Figure 7 shows time series of two metrics for the second scenario. On the horizontal axis, we plot the simulation time and on the vertical axis the corresponding metric RSS or PDR. Note that for both plots the data points do not start exactly at simulation time 0 s, that is due to the delayed insertion of the second vehicle in the scenario to establish the 80 m distance.

Since the initial road segment is perfectly straight and the inter-vehicle distance is static, we observe a constant RSS of -93 dBm. This matches exactly the 80 m value from Figure 1a. Similarly, the PDR indicates 100 % probability of reception, which fits with the plot of H2 at 0° in Figure 5. This pattern holds for all straight road segments.

At around 140 s, the vehicles go through the first turn, turning right. When driving through the turn, the RSS increases

yet fluctuates. That is because while on the turn H1 falls on the right side of the radiation pattern of V0's headlight. In Figure 1a, we saw that the headlight has higher concentration of power on that side, thus the improved RSS. Regarding the fluctuations, they occur due to intermittent changes in the angle and the distance between V0 and H1. Looking at the PDR, we do not observe any changes for the same timespan. This confirms our expectations: Because the RSS only got better, whereas the PDR was at 100% already.

The next interesting point in the simulation is when the vehicles go through the left turn. Here, the metrics behave opposite of what happened in the first turn. The RSS drops to -100 dBm because now the H1 is on the left of V0's headlight and the radiation power is lower. In the left turn, the changes in RSS are reflected also in the PDR. First, the PDR changes drastically falling to 0%. Then it starts fluctuating between 0-100%. These extreme values occur because as the vehicles drive on the turn the SNR changes between 5-30 dB; this range includes the steep curve of the lower plot in Figure 4.

As can be seen from the presented results, straight LOS communication is not the limiting factor in most cases. Yet, as soon as the road bends and cars have to go through curves, the connectivity very much depends on (a) the angle of the curve and (b) the direction of the turn. Protocol and application designers need to consider such facts, e.g., by anticipating such behavior based on mobility and map information.

VI. CONCLUSION

We presented a novel Open Source empirical model for estimating the Received Signal Strength (RSS) and eventually the Packet Delivery Ratio (PDR) of Visible Light Communication (VLC) communication in vehicular environments. The model is based on a number of real world experiments. Using curve fitting methods, we were able to derive an analytical model that can, in combination with the raw measurement data, be implemented in state-of-the-art simulation tools. We choose the Open Source Veins simulator for this integration and subsequent simulation experiments, because it is widely used in the vehicular networking research community. Based on this model, we performed a number of experiments to shed more light into the effects of Vehicular VLC (V-VLC). We were particularly interested in the resulting performance of VLC communication between cars on the same lane as well as to cars on parallel lanes. For this, we studied the impact of the angle of the communication. In conclusion, it can be said that our novel path loss model for V-VLC helped confirming a number of interesting effects due to the very special light radiation pattern of modern cars' headlight modules. In a second step, we investigated the impact of turns on a curved road on the VLC communication. We have seen that the specific radiation pattern of car headlights may cause problems in maintaining a stable VLC link between two cars, particularly when turning left (that is to say right in countries with left lane traffic). With the results of simulations from our scenarios we see that our tool can successfully simulate various aspects of the Physical Layer (PHY) for V-VLC.

REFERENCES

- [1] T. Komine and M. Nakagawa, "Fundamental analysis for visible-light communication system using LED lights," *IEEE Transactions on Consumer Electronics*, vol. 50, no. 1, 100-107, Feb. 2004.
- [2] "IEEE Standard for Local and metropolitan area networks - Part 15.7: Short-Range Wireless Optical Communication Using Visible Light," IEEE, Std 802.15.7-2011, Sep. 2011.
- [3] N. Lourenco, D. Terra, N. Kumar, L. N. Alves, and R. L. Aguiar, "Visible Light Communication System for outdoor applications," in *8th International Symposium on Communication Systems, Networks & Digital Signal Processing (CSNDSP 2012)*, Poznan, Poland, Jul. 2012.
- [4] C. B. Liu, B. Sadeghi, and E. W. Knightly, "Enabling Vehicular Visible Light Communication (V2LC) Networks," in *8th ACM International Workshop on Vehicular Internet Networking (VANET 2011)*, Las Vegas, NV: ACM, Sep. 2011, 41-50.
- [5] M. Uysal, Z. Ghassemlooy, A. Bekkali, A. Kadri, and H. Menouar, "Visible Light Communication for Vehicular Networking: Performance Study of a V2V System Using a Measured Headlamp Beam Pattern Model," *IEEE Vehicular Technology Magazine*, vol. 10, no. 4, pp. 45-53, Dec. 2015.
- [6] M. Segata, R. Lo Cigno, H.-M. Tsai, and F. Dressler, "On Platooning Control using IEEE 802.11p in Conjunction with Visible Light Communications," in *12th IEEE/IFIP Conference on Wireless On demand Network Systems and Services (WONS 2016)*, Cortina d'Ampezzo, Italy: IEEE, Jan. 2016, pp. 124-127.
- [7] S.-H. Yu, O. Shih, H.-M. Tsai, N. Wisitpongphan, and R. Roberts, "Smart automotive lighting for vehicle safety," *IEEE Communications Magazine*, vol. 51, no. 12, pp. 50-59, Dec. 2013.
- [8] J. Classen, D. Steinmetzer, and M. Hollick, "Opportunities and pitfalls in securing visible light communication on the physical layer," in *3rd ACM Workshop on Visible Light Communication Systems (VLCS 2016)*, New York, NY: ACM, Oct. 2016, pp. 19-24.
- [9] Y. Wang, X. Huang, L. Tao, and N. Chi, "1.8-Gb/s WDM Visible Light Communication Over 50-meter Outdoor Free Space Transmission Employing CAP Modulation and Receiver Diversity Technology," in *Optical Fiber Communication Conference*, Los Angeles, CA: OSA, Mar. 2015.
- [10] H.-Y. Tseng, Y.-L. Wei, A.-L. Chen, H.-P. Wu, H. Hsu, and H.-M. Tsai, "Characterizing link asymmetry in vehicle-to-vehicle Visible Light Communications," in *7th IEEE Vehicular Networking Conference (VNC 2015)*, Kyoto, Japan: IEEE, Dec. 2015, pp. 88-95.
- [11] C. Sommer, R. German, and F. Dressler, "Bidirectionally Coupled Network and Road Traffic Simulation for Improved IVC Analysis," *IEEE Transactions on Mobile Computing*, vol. 10, no. 1, pp. 3-15, Jan. 2011.
- [12] P. Luo, Z. Ghassemlooy, H. Le Minh, E. Bentley, A. Burton, and X. Tang, "Performance analysis of a car-to-car visible light communication system," *Applied Optics*, vol. 54, no. 7, pp. 1696-1706, Mar. 2015.
- [13] B. Turan, O. Narmanlioglu, S. Coleri Ergen, and M. Uysal, "Broadcasting brake lights with MIMO-OFDM based vehicular VLC," in *8th IEEE Vehicular Networking Conference (VNC 2016)*, Columbus, Ohio: IEEE, Dec. 2016.
- [14] A.-L. Chen, H.-P. Wu, Y.-L. Wei, and H.-M. Tsai, "Time variation in vehicle-to-vehicle visible light communication channels," in *8th IEEE Vehicular Networking Conference (VNC 2016)*, Columbus, Ohio, Dec. 2016.
- [15] F. Miramirghani, O. Narmanlioglu, M. Uysal, and E. Panayirci, "A Mobile Channel Model for VLC and Application to Adaptive System Design," *IEEE Communications Letters*, 2017.
- [16] S. Ishihara, R. V. Rabsatt, and M. Gerla, "Improving Reliability of Platooning Control Messages Using Radio and Visible Light Hybrid Communication," in *7th IEEE Vehicular Networking Conference (VNC 2015)*, Kyoto, Japan: IEEE, Dec. 2015, pp. 96-103.
- [17] T. Yamazato, A. Ohmura, H. Okada, T. Fujii, T. Yendo, S. Arai, and K. Kamakura, "Range Estimation Scheme for Integrated I2V-VLC using High-Speed Image Sensor," in *IEEE International Conference on Communications (ICC), 2nd Workshop on Optical Wireless Communications*, Kuala Lumpur, Malaysia: IEEE, May 2016.
- [18] N. Kumar, N. Lourenço, D. Terra, L. N. Alves, and R. L. Aguiar, "Visible Light Communications in Intelligent Transportation Systems," in *IEEE Intelligent Vehicles Symposium (IV 2012)*, Alcalá de Henares, Spain: IEEE, Jun. 2012.